JOURNAL OF MATERIALS SCIENCE 26 (1991) 2300–2304

Measurement of stress in nickel oxide layers by diffraction of synchrotron radiation

A. N. FITCH
Department of Chemistry, University of Keele, Staffordshire ST5 5BG, UK
C. R. A. CATLOW
The Royal Institution of Great Britain, 21 Albemarle Street, London W1X 4BS, UK
A. ATKINSON
Materials Chemistry Department, AEA Technology, Harwell Laboratory, Didcot, Oxfordshire OX11 0RA, UK

The average in-plane stress in a number of polycrystalline NiO thermal oxidation scales has been measured by the $\sin^2\psi$ technique at the Synchrotron Radiation Source, Daresbury, using the high-resolution diffractometer 8.3, which exploits parallel-beam X-ray optics. There are a number of distinct advantages for stress measurements using this arrangement. Shifts in peak positions of much less than 0.005° can be accurately measured, and the tunability of the incident radiation allows control over the depth of penetration of the X-rays into the surface of the specimen.

1. Introduction

Stress in an oxide scale grown by thermal oxidation on a metal substrate is seen as an important factor in determining the practical adhesion of the oxide layer to the metal. High stress can lead to spallation of the scale leaving bare metal where renewed oxidation or corrosion can occur. The stress may originate from the mismatch between the crystal lattices of the scale and the metal substrate (epitaxial stress), from differential rates of thermal contraction on cooling, or from the oxidation process itself.

Measurement of stress by the $\sin^2\psi$ technique is well established [1–3]. The position of a diffraction peak is measured initially with the sample in $\theta/2\theta$ geometry. In this orientation the spacing between lattice planes parallel with the surface is measured. The sample is then rotated by an angle ψ about the diffractometer axis and the position of the peak measured again. The spacing between lattice planes at an angle ψ to the surface is now being probed. If there are stresses acting in the surface layer then a larger component of the stress acts perpendicular to the diffracting planes as $|\psi|$ increases, and a shift in the position of the peak occurs. In the absence of shear stresses and a stress gradient with depth, a linear variation of 2θ with $\sin^2\psi$ is observed for both positive and negative ψ tilts, i.e.

$$\Delta 2\theta = \frac{360}{\pi} \tan\theta \frac{1+\nu}{E} \sigma \sin^2\psi \qquad (1)$$

where ν is Poisson's ratio, E is Young's modulus, and σ is the in-plane stress [3].

Hence from a plot of 2θ versus $\sin^2\psi$ the in-plane stress can be determined, provided Young's modulus and Poisson's ratio are known for the material under investigation. If there is significant variation of the stress with depth, curvature of the plot will be observed, because the depth of penetration of the X-rays varies with ψ. The variation of the depth of 50% penetration with scale thickness and sample orientation, ω, is shown in Fig. 1 for the 400 reflection of NiO. (50% penetration is the depth from above which 50% of the diffracted radiation originates.) The depth of penetration is identical for positive and negative ψ tilts and is a maximum when ψ is zero, i.e. in $\theta/2\theta$ geometry when $\omega = \theta$. If shear stresses are present then $\Delta 2\theta$ will be different for positive and negative ψ tilts leading to "ψ splitting" in the plots.

The high-resolution powder diffractometer 8.3 at Daresbury has been fully described elsewhere [4, 5]. The diffractometer has precision encoders mounted directly on the sample (ω) and detector (2θ) axes, with a nominal precision of 1×10^{-3} and 1×10^{-4} degrees, respectively. A schematic diagram is shown in Fig. 2. The instrument operates with parallel beam geometry and uses a flat-plate specimen. The high resolution is largely controlled by the action of the long, fine, diffracted-beam collimators [6]. Owing to the parallel nature of synchrotron radiation in the vertical sense, the collimators define precisely the angle through which the scattered radiation must be deflected in order to enter the detector. For well-crystallized samples full widths at half maximum (FWHM) of 0.05–0.06° are usual on 8.3 (compared with around 0.15° for a conventional diffractometer in $\theta/2\theta$ geometry), although for the NiO scales somewhat broader peaks are observed depending on the thickness of the scale.

0022–2461/91 $03.00 + .12

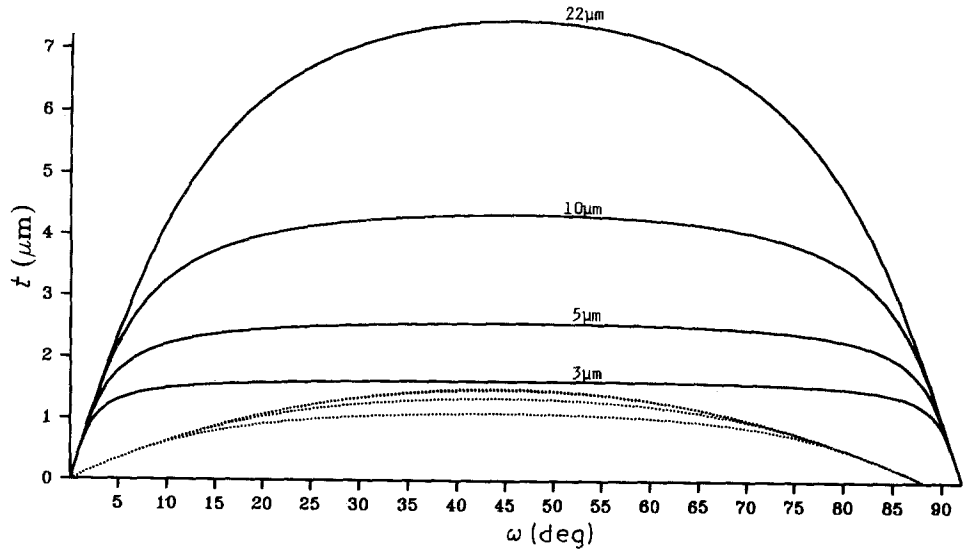

Figure 1 Depth of 50% penetration (t) as a function of sample orientation (ω) of X-rays into NiO scales of various thicknesses between 3 and 22 μm for the 400 reflection of NiO (d_{400} = 0.10421 nm). The calculation is illustrated at two wavelengths above and below the NiK absorption edge (0.1488 nm); (——) λ = 0.150 nm, 2θ = 92.060°, μ = 260 cm^{-1}; (· · ·) λ = 0.145 nm, 2θ = 88.168°, μ = 1607 cm^{-1}. The relationship between θ, ω and ψ is $\omega = \theta + \psi$.

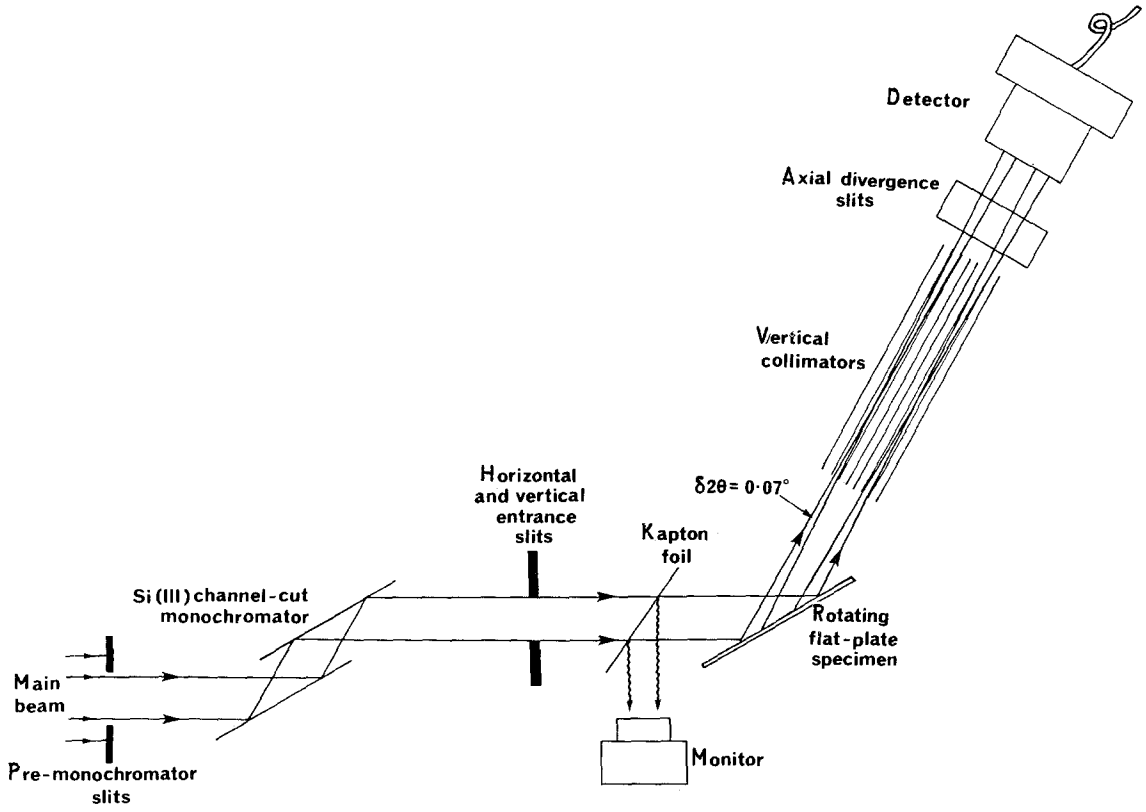

Figure 2 Schematic diagram of the high-resolution powder diffractometer 8.3 at the Synchrotron Radiation Source, Daresbury.

2. Advantages of synchrotron radiation

There are a number of distinct advantages of performing surface stress measurements with a diffractometer of the design of 8.3 with parallel-beam optics as compared with a conventional focusing Bragg–Brentano diffractometer.

1. The narrow widths of the diffraction peaks, the precision encoder system and the well-defined peak-shape function mean that peak centroid location is possible to a precision as high as 0.0001° for well-crystallized samples. Very tiny shifts in peak position can easily be measured.

2. The high intensity of the incident beam leads to reasonable counting times for data acquisition. The sensitivity of the position of a diffraction peak to a change in lattice spacing is greatest at high values of 2θ, unfortunately where the form-factor for X-ray scattering is smallest.

3. Owing to the parallel-beam optics, the position of a diffraction peak is not sensitive to misalignment of the diffractometer or the positioning of the sample. In conventional, focusing geometry, peak shifts are observed if the sample is not positioned exactly on the axis of 2θ, and further small shifts occur as the depth of penetration of the X-rays into the sample varies with sample orientation.

4. There are no problems with loss of focusing when the sample is rotated from $\theta/2\theta$ geometry. With

conventional diffractometers, significant peak broadening accompanies the application of the ψ tilts. On 8.3 the peak shape hardly changes with sample orientation, as illustrated in Fig. 3.

5. The incident radiation is monochromatic; there are no problems with $\alpha_1\alpha_2$ doublets.

6. By changing the wavelength, the depth of penetration can be controlled. Fig. 1 shows the change in penetration depth for the 4 0 0 reflection of NiO at 0.150 and 0.145 nm, i.e. just above and just below the Ni*K* absorption edge. Hence variation of stress with depth can be more readily investigated.

These attributes should allow stress measurements to be performed with a much lower level of systematic error than has so far been possible.

3. Experimental procedure

Coupons of 0.5 mm thick Ni foil (Puratronic, 30 p.p.m. maximum impurity level) were cut into squares of side 1 cm or 2.5 cm. The surface was polished to a mirror finish, then the coupon was annealed *in vacuo*, polished to 1 μm with diamond paste, then oxidized at 700 or 800 °C. The change in mass indicated an oxide thickness of 22.7, 10.4 and 5.7 μm for the 1 cm square samples, and 13.7, 9.3 and 6.4 μm for the 2.5 cm square samples.

Scans of the diffraction peaks from the scales and from pure NiO powder at a wavelength of 0.155 nm revealed a complex peak shape due to the small rhombohedral distortion of the cubic rock-salt structure of NiO below its Néel temperature (522 K) [7, 8], which is visible with the high resolution of 8.3, Fig. 4. The composite peak shape greatly complicates the location of the centroid of the peaks, so that stress measurements were performed using the 4 0 0 reflection, which is not split by the rhombohedral distortion. At 0.155 nm this peak is close to 96.2° and peak shifts with changes in sample orientation are very small, about 0.04° 2θ at the maximum ψ tilts. Such small shifts are easily measured, however, using 8.3.

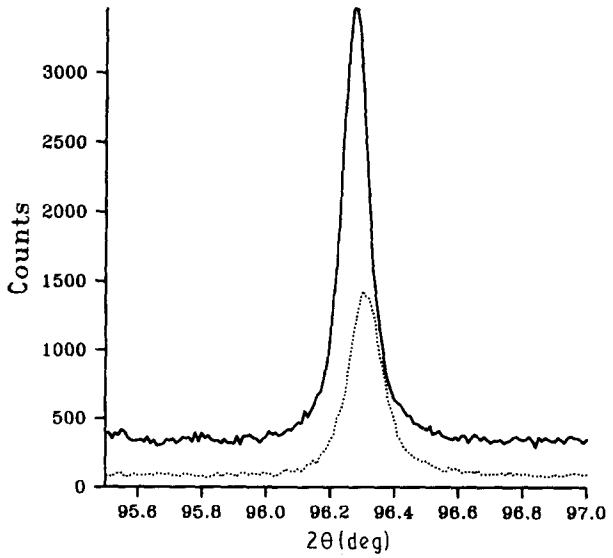

Figure 3 The 4 0 0 peak from a 22.7 μm NiO scale at (——) $\psi = 0°$ and (· · · ·) $\psi = 40°$. The peak width does not vary with ψ. The sensitivity of the 8.3 diffractometer to tiny peak shifts is apparent. The decrease in the peak intensity at $\psi = 40°$ is due to the decrease in the volume of the sample irradiated at positive ψ tilts.

Stress measurements were performed by the $\sin^2\psi$ method at wavelengths of 0.155 and 0.145 nm for the 2.5 cm square samples, and at 0.155 nm only for the 1 cm square samples. The high fluorescence background at the shorter wavelength meant that data of sufficient statistical quality could not be obtained for the smaller samples in a reasonable counting time. Data were collected in steps of 0.01° 2θ over the range of the 4 0 0 reflection. Peak positions were obtained by least-squares fitting of a pseudo-Voigt peak shape and a linear background to the measured intensities.

4. Results

Typical results showing the variation of the position of the 4 0 0 peak with $\sin^2\psi$ for the 1 cm square samples are illustrated in Fig. 5 for samples with oxide thicknesses of 5.7 and 22.7 μm. There is evidence for modest ψ splitting suggesting a small degree of shear stress. The positive slopes of the lines indicate that the lattice spacings are decreasing as $|\psi|$ increases, i.e. the NiO layers are under compression, as has been observed by other workers [9]. With ν taken as 0.416 and E as 9.56×10^4 MPa [10], average in-plane stresses were calculated and are reported in Table I. A realistic estimate of the confidence limits on these values is probably about $\pm$ 5 MPa, with the main uncertainty arising from the simple assignment of an average in-plane stress for a system showing signs of shear stresses. These average in-plane stresses are lower than those reported in a similar study using conventional X-ray diffractometry, where in-plane stresses of up to $-$ 400 MPa were observed [9], though a factor of around 2.5 can be attributed to a different choice E and ν. Pivin *et al.* [9] have used $E = 2.2 \times 10^5$ MPa, $\nu = 0.3$, which are values appropriate for NiO above its Néel temperature in the cubic phase [10, 11], whereas the high resolution of 8.3 shows that the NiO layers in our samples are rhombohedrally distorted.

There is no apparent correlation between the stresses and the layer thickness in the above measurements. The highest stress appears to be in the thinnest scale where the X-rays are penetrating closer to the oxide/substrate interface where stresses would be expected to be highest. A method to assess whether the high stress in the 5.7 μm sample arises from stress close to the interface would be to attempt the experiment at 0.145 nm just below the Ni*K* edge where the depth of penetration of the X-rays into the samples is reduced. This was not, however, practicable for the 1 cm square samples as explained above.

For the 2.5 cm square samples the average in-plane stresses are also reported in Table I. At 0.155 nm the variation of the stress with oxide thickness mirrors the pattern seen for the smaller samples with the highest stress seen in the thinnest scale. At 0.145 nm the measurements were more difficult, with a high background due to fluorescence, so that longer counting times were needed at each step. Furthermore, at positive ψ tilts the diffraction peaks become very weak

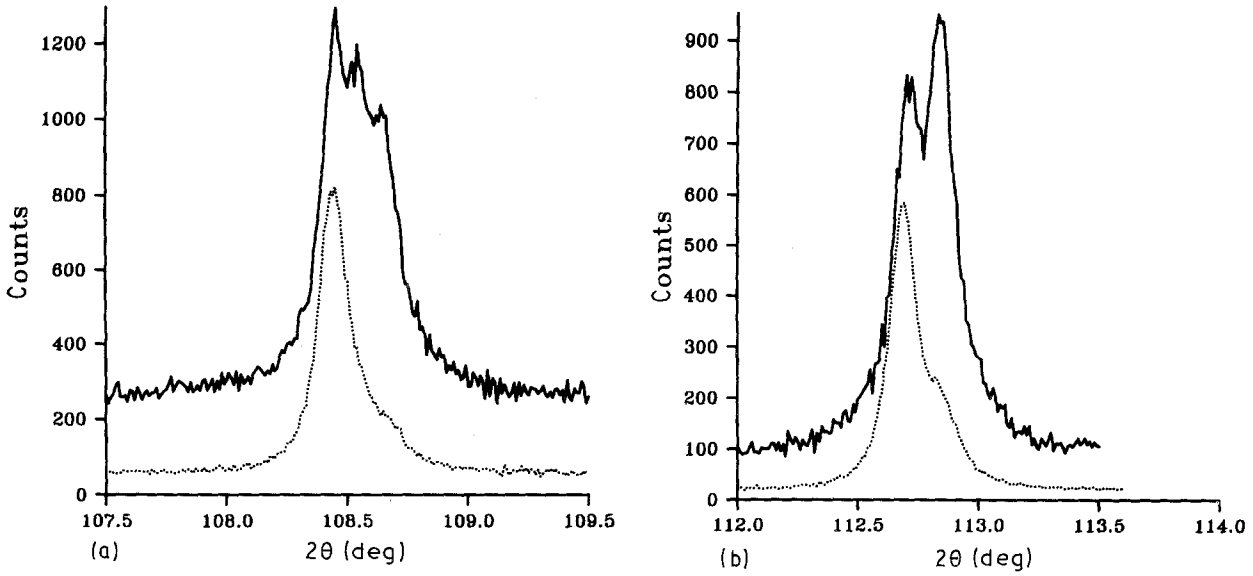

Figure 4 Scans of (a) the 3 3 1 and (b) the 4 2 0 peaks from pure NiO powder and a 22.7 μm NiO scale. (——) Pure NiO sample, (· · · ·) NiO scale. The differences in the relative intensities of the components of the peaks for the powder and the scale indicate texture in the scale.

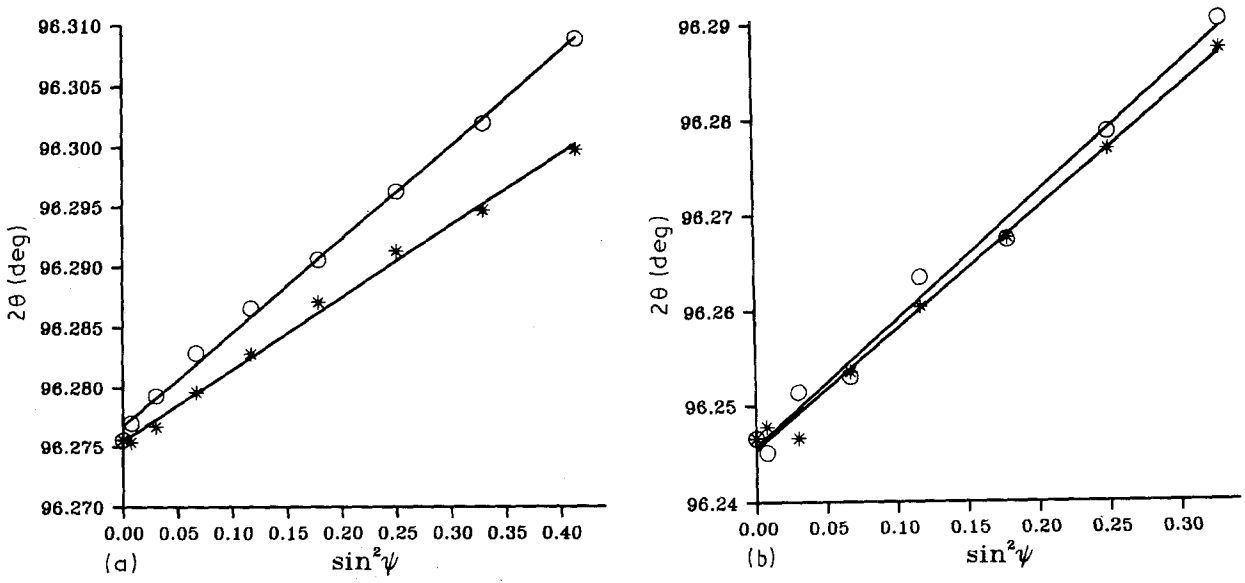

Figure 5 Variation of the peak position (2θ) with $\sin^2\psi$ for the 4 0 0 peak of NiO scales of thickness (a) 22.7 μm and (b) 5.7 μm. (○) ψ positive, (*) ψ negative. The best least-squares straight-line fits are also shown.

TABLE I Average in-plane stresses for NiO scales of various thicknesses and sizes determined at wavelengths of 0.155 and 0.145 nm

Scale thickness (μm)	Sample size (cm^2)	Average stress with λ = 0.155 nm (MPa)	Average stress with λ = 0.145 nm (MPa)
22.7	1 × 1	− 38	–
10.4	1 × 1	− 28	–
5.7	1 × 1	− 69	–
13.7	2.5 × 2.5	− 37	− 34
9.3	2.5 × 2.5	− 20	− 20
6.4	2.5 × 2.5	− 48	− 30

because the volume of the scale irradiated is diminished. At negative ψ tilts the peaks are much stronger and the results were considered more reliable for these scans. A typical diffraction profile is shown in Fig. 6.

At 0.145 nm there is possibly a slight decrease in the stress in the two thicker scales, suggesting some drop in the stresses towards the surface of the samples. However, the most significant drop is for the 6.4 μm sample. This would support the idea that the stresses in the interfacial region are more severe, and contribute significantly to the high stress seen in the thinnest samples.

5. Conclusions

The advantages of using synchrotron radiation and parallel-beam optics for surface stress measurements by the $\sin^2\psi$ method have been of great benefit in the

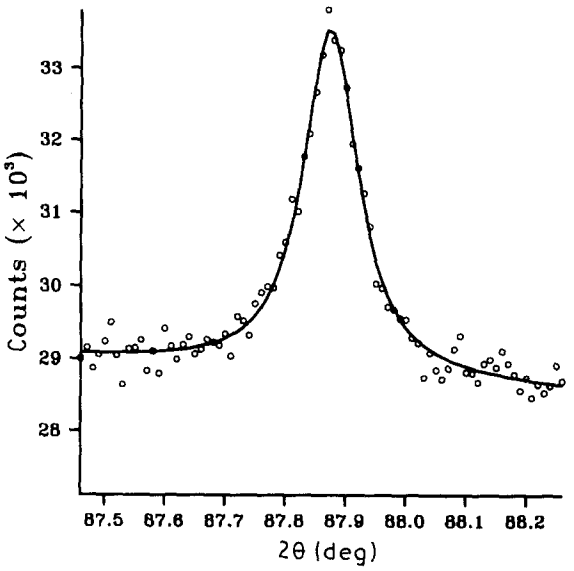

Figure 6 Fit of a pseudo-Voigt peak shape and a linear background to the 400 peak of a 13.7 μm NiO scale at $\lambda = 0.145$ nm, with $\psi = -15°$.

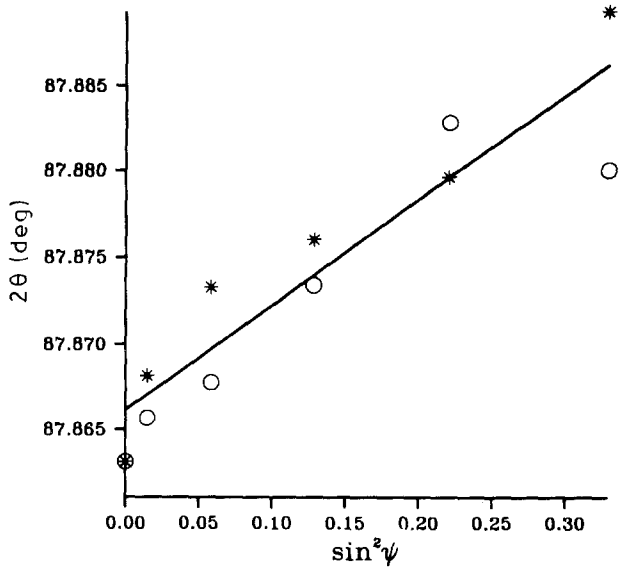

Figure 7 Variation of the peak position (2θ) with $\sin^2\psi$ for the 400 peak of a 13.7 μm NiO scale at $\lambda = 0.145$ nm; (○) ψ positive, (*) ψ negative. A single straight line has been fitted to the points.

study of stress in NiO scales. Owing to the rhombohedral distortion of NiO it has been necessary to use the 400 diffraction peak for the stress measurements, as all higher angle peaks are composite. The 400 peak is close to 96.2° 2θ, a relatively low angle for stress measurements, and the stresses seen in the scales are not large, generally less than 70 MPa. Very small shifts in peak position with changes in ψ are therefore seen. Small shifts of less than 0.005° have, however, been easily and accurately measured using the 8.3 diffractometer. The stresses observed are much lower than those reported by other workers using conventional X-ray diffractometry [9], although a factor of around 2.5 is due to a choice of Young's modulus and Poisson's ratio appropriate to NiO in the rhombohedral phase below the Néel temperature [10].

The highest stress is observed in the thinnest scales, in which the X-rays penetrate closer to the interface between the scale and the metal substrate, where stresses would be expected to be highest. Evidence supporting this supposition comes from the apparent reduction in the stress when the depth of penetration of the X-rays into the surface is reduced by changing the wavelength to just below the Ni*K* absorption edge. By tuning the wavelength between 0.145 and 0.150 nm (simply by rotation of the instrument's monochromator), any depth of penetration may be selected between the limits illustrated in Fig. 1. Whilst routine stress measurements will continue to be carried out successfully using conventional X-ray sources, this control over the depth of penetration of the X-rays is a major advantage of using synchrotron radiation for stress measurements and will be of great importance for characterizing systems where there is a significant variation of the stress with depth.

Acknowledgements

The authors thank the SERC Daresbury Laboratory for the provision of the beam time on the 8.3 diffractometer, and are grateful to R. J. Cernik and P. Pattison, Daresbury, for experimental assistance and useful discussions. We also thank A. Jones and A. W. Harris, Harwell Laboratory, for useful discussions and sample preparation, respectively.

References

1. I. C. NOYAN and J. B. COHEN, "Residual Stress, Measurement by Diffraction and Interpretation" (Springer-Verlag, New York, 1987) Ch. 5.
2. I. C. NOYAN, *Metall. Trans.* **14A** (1983) 249.
3. D. LONSDALE, *J. Appl. Crystallogr.* **19** (1986) 300.
4. W.PARRISH and M. HART, *Z. Kristallogr.* **179** (1987) 161.
5. R. CERNIK, P. PATTISON, P. MURRAY, C. R. A. CATLOW and A. FITCH, *SERC Bull.* **3** (12) (1988) 14.
6. R. J. CERNIK, P. K. MURRAY, P. PATTISON and A. N. FITCH, *J. Appl. Crystallogr.* **23** (1990) 292.
7. G. A. SLACK, *J. Appl. Phys.* **31** (1960) 1571.
8. F. FIEVET, P. GERMI, F. DE BERGEVIN and M. FIGLARZ, *J. Appl. Crystallogr.* **12** (1979) 387.
9. J. C. PIVIN, J. MORVAN, D. MAIREY and J. MIGNOT, *Scripta. Metall.* **17** (1983) 179.
10. M. R. NOTIS, R. M. SPRIGGS and W. C. HAHN, *J. Geophys. Res.* **76** (1971) 7052.
11. V. KRISHNAMACHARI and M. R. NOTIS, *Acta Metall.* **25** (1977) 1307.

Received 27 March
and accepted 2 August 1990